Exp. Anim. 67(2), 249–257, 2018

—Original—

Grading fatty liver by ultrasound time-domain radiofrequency signal analysis: an *in vivo* study of rats

Wenwu LING[1)], Jierong QUAN[2)], Jiangli LIN[3)], Tingting QIU[1)], Jiawu LI[1)], Qiang LU[1)], Changli LU[4)], and Yan LUO[1)]

[1)]*Department of Ultrasound, West China Hospital of Sichuan University, No. 37 Guo Xue Xiang, Chengdu, Sichuan 610041, P.R. China*
[2)]*Department of Ultrasound, Sichuan Academy of Medical Science & Sichuan Provincial People's Hospital, No. 32 Yi Huan Lu Xi Er Duan, Chengdu, Sichuan 610041, P.R. China*
[3)]*Department of Biomedical Engineering, Sichuan University, Wangjiang Campus, No. 11 Yi Huan Lu Nan San Duan, Chengdu, Sichuan 610041, P.R. China*
[4)]*Department of Pathology, West China Hospital of Sichuan University, No. 37 Guo Xue Xiang, Chengdu, Sichuan 610041, P.R. China*

Abstract: This study aimed to assess the severity of fatty liver (FL) by analyzing ultrasound radiofrequency (RF) signals in rats. One hundred and twenty rats (72 in the FL group and 48 in the control group) were used for this purpose. Histological results were the golden standard: 42 cases had normal livers (N), 30 cases had mild FL (L1), 25 cases had moderate FL (L2), 13 cases presented with severe FL (L3), and 10 cases were excluded from the study. Four RF parameters (Mean, Mean/SD ratio [MSR], skewness [SK], and kurtosis [KU] were extracted. Univariate analysis, spearman correlation analysis, and stepwise regression analysis were used to select the most powerful predictors. Receiver operating characteristic (ROC) analysis was used to compare the diagnostic efficacy of single indexes with a combined index (Y) expressed by a regression equation. Mean, MSR, SK, and KU were significantly correlated with FL grades (r=0.71, P<0.001; r=0.81, P<0.001; r=−0.79, P<0.001; and r=−0.74, P<0.001). The regression equation was $Y=-4.48 + 3.20 \times 10^{-2}X1 + 3.15X2$ (P<0.001), where Y=hepatic steatosis grade, X1 =Mean, and X2 =MSR. ROC analysis showed that the curve areas of the combined index (Y) were superior to simple indexes (Mean, MSR, SK, and KU) in evaluating hepatic steatosis grade, and they were 0.95 (L≥L1), 0.98 (L≥L2), and 0.99 (L≥L3). Ultrasound radiofrequency signal quantitative technology was a new, noninvasive, and promising sonography-based approach for the assessment of FL.

Key words: fatty liver, rat, ultrasound radiofrequency signal

Introduction

The worldwide prevalence of fatty liver (FL) has shown an increase recent changes in lifestyle [1]. FL is histologically defined as the accumulation of more than 5% to 10% fat in the liver. Steatosis, infiltration of fat into liver cells, is one of the main histological features of FL, and it is associated with disturbance of the me-

(Received 9 October 2017 / Accepted 8 December 2017 / Published online in J-STAGE 12 January 2018)
Address corresponding: Y. Luo, Department of Ultrasound, West China Hospital of Sichuan University, No. 37 Guo Xue Xiang, Chengdu, Sichuan 610041, P.R. China

tabolism caused by obesity, diabetes, hyperlipidemia, and so on [4]. Mild FL is considered to be a reversible entity, while moderate and severe FL may progress through steatohepatitis to cirrhosis and even to hepatocellular carcinoma [11]. Additionally, an individual with mild FL can be a safe liver donor in liver transplantation, while moderate and severe FL may increase the risk of postoperative complications and graft failure [15].Therefore, there is growing demand for early diagnosis and accurate assessment of FL.

Several imaging modalities, including ultrasonography (US), X-ray computed tomography (CT), and magnetic resonance imaging (MRI) have been used to assess FL. However, they have shown their own limitations in terms of accurate grading of FL [17]. Currently, US imaging is the first-line image modality to detect and grade FL [17]. However, it has less sensitivity in diagnosing mild FL, and it is subjective in grading FL [5, 7]. CT provides high performance in qualitative diagnosis of moderate to severe FL, but its diagnostic performance for quantitative assessment of FL is not clinically acceptable by all people. Moreover, it exposes the subjects to ionizing radiation [14].Recently, MRI has shown good prospects in quantitative assessment of FL, but MRI examinations are expensive and time-consuming [20, 24]. Liver biopsy has high accuracy in diagnosing and grading FL, but it is limited by its invasive characteristics. Thus it is still a challenge to diagnose FL early and grade FL accurately in clinical practice.

The subjectivity in ultrasound grading of FL is mainly due to the influences of instrument settings, operator experience, and various patient conditions [5]. To evaluate FL more accurately, US image texture analysis has been used, and some achievements have been made [12]. Studies performing US image texture analysis are based on analysis of video signals. Compared with ultrasound video signals, the original RF signals are raw data without much signal processing. In theory, such RF signals would contain more information for better characterizing the tissue than gray-scale images. In previous studies, quantitative features extracted directly from the original RF signals have been suggested for comparison of ultrasound and liver pathological findings in steatosis, fibrosis, and cirrhosis [2, 9, 18, 22]. These studies showed that ultrasound RF features were correlated with liver pathological changes. However, up to our knowledge, there are few papers that have focused on grading FL by utilizing ultrasound RF signal-based methods.

In this study, we firstly established a rat model with different FL stages and then extracted four quantitative statistic features from the ultrasound time-domain RF signals. To diagnose and grade FL, we set up a correlative regression equation with the most powerful predictors. This study also evaluated the diagnostic performance of the four parameters in various degrees of FL.

Materials and Methods

Materials

This study was approved by the Animal Ethics Committee of the Animal Facility of West China Hospital. One hundred and twenty male Wistar rats provided by the Laboratory Animal Center of Sichuan University were used in this study. The rats were handled according to the University and Animal Ethics Committee Guidelines of the Animal Facility of West China Hospital. The rats were randomly divided into 2 groups: the control group (n=48) and experimental group (n=72). Each rat weighed approximately 250 ± 20 g, all the rats were 8 weeks of age, and there was no significant difference in body weight among the two groups. The rats in the experimental group were fed with a high fat diet composed of 10% lard, 2% cholesterol, 0.1% pig bile salt, and 87.9% normal food, while the rats in the control group were given free access to normal food and water.From the 5th to 16th week, performed the experiments 12 times in total;6 experimental group rats and 4 control group rats were chosen randomly for B-mode ultrasound scanning and RF signals acquisition in vivo on the same day of each week. All rats were anesthetized with an intraperitoneal injection of ketamine (70 mg/kg) and xylazine (10 mg/kg) and then placed in the supine position with whole thorax abdominal skin preparation. Then they were sacrificed by cervical dislocation, and a histological examination was performed. All examinations were performed after the rats had fasted for 8–12 h.

Ultrasonic RF signal acquisition

A Siemens Antares system (Siemens Healthcare, Mountain View, CA, USA), equipped with an Axius Direct Ultrasound Research Interface (URI), was used to acquire the RF signals. A system provides 16 bit digitized echo signals at a sampling rate of 40 MHz. A VFX13-5 probe with a center frequency of 11.43 MHz was utilized to scan the rats. In the data acquisition process, the scanning settings were 35 dB/65 dB, 2.5 cm,

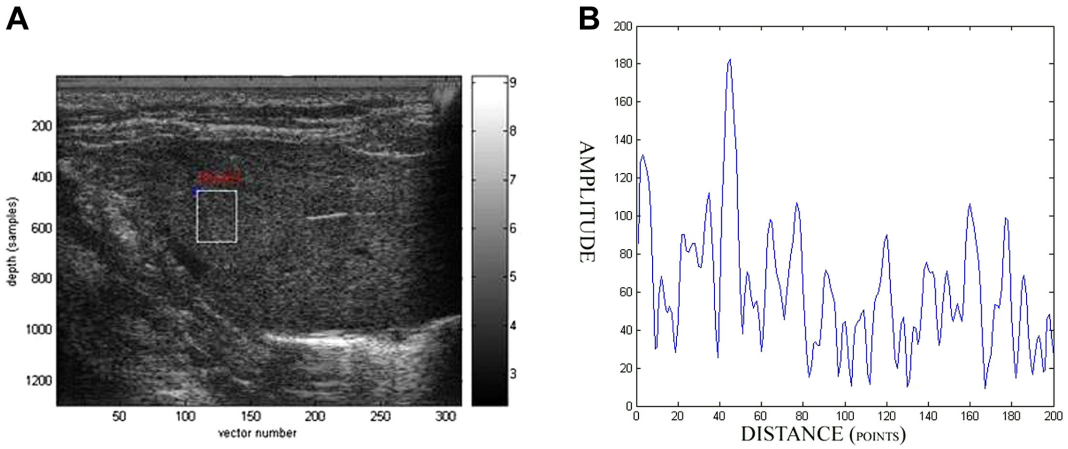

Fig. 1. The envelope data in the region of interest (ROI). a) A 2-D sonographic image constructed by MATLAB 7.0 from the radiofrequency signals and ROI localization. In this figure, 1250 samples on the Y-axis corresponds to 2.5 cm. b) The envelope data of a digitized time-domain signal of a line in the ROI.

and 0.7 for gain, depth, and MI, respectively. RF data for the whole image range (with a 2.5 cm depth) were acquired. For each rat, two frames of RF data were used for analysis. All the RF data were stored on a hard disk for subsequent offline analysis.

Feature extraction of ultrasonic RF signals

The RF signals were analyzed with commercially available data processing software (MATLAB 7.0, The Mathworks Inc., Natick, MA, USA). The region of interest (ROI) was rectangle in shape with 30 × 200 pixels (Fig. 1A). It was set at 1 cm below the liver surface within the liver parenchyma. It was adjusted in such a way that it avoided major intrahepatic blood vessels and bile ducts. First, the envelope of each signal line of the ROI was obtained by the Hilbert transform (Fig. 1B), then the statistical parameters, i.e., the Mean, Mean/SD ratio (MSR), skewness (SK), and kurtosis (KU), were calculated from the envelope, and finally the values of these parameters for each vector were averaged for all vectors of the liver ROI in Fig. 1A. The three parameters were defined as shown in equations (1) to (3) [8].

$$\mathrm{MSR} = \frac{\mu}{\sigma}, \qquad (1)$$

$$\mathrm{SK} = \frac{E\left[\left(s(t)-\mu\right)^3\right]}{\sigma^3}, \qquad (2)$$

$$\mathrm{KU} = \frac{E\left[\left(s(t)-\mu\right)^4\right]}{\sigma^4}, \qquad (3)$$

where $s(t)$ is the envelope of the original radiofrequency signal, μ is the mean of the envelope population, and σ is the standard deviation of the envelope population.

Three ROIs were set for each frame, and six ROIs were set for each rat. Therefore, the four primary statistics of each rat were measured six times, and each mean was taken to represent the rat.

Histological study

After the rats were sacrificed by cervical dislocation, histopathology examinations were carried out to grade the FL degree. A cubic liver tissue specimen with size of about 10 mm × 10 mm × 10 mm was sampled at the same place of US scanning for each rat. The tissue specimens were stained with hematoxylin and eosin (H&E). The FL grade was independently evaluated by two experienced pathologists according to the percentage of fat-occupying hepatocytes: normal, no fatty liver; mild, less than 33%; moderate, 33–66%; and severe, more than 66% [23]. The final diagnosis was the consensus of the two pathologists.

Statistical analysis

The SPSS 13.0 software was used for statistical analysis. Four RF signal features (Mean, MSR, SK, and KU) were expressed as the mean ± SD. To analyze the difference in different groups, the one-way analysis of variance, univariate analysis, and least significant difference test were used. The Spearman rank correlation coefficient was used for the correlations analysis. In order to improve the diagnostic efficacy of the grade of hepatic steatosis, a stepwise regression equation combining ap-

plication of the most powerful predictors was determined. Receiver operating characteristic (ROC) analysis was used to compare the diagnostic efficiency of single indexes and the combined index expressed by the regression equation. Cutoff values were defined prediction regions for each FL stage. Area under the ROC curve (AUC), sensitivity, and specificity were calculated with the optimal cutoff values that maximized the Youden's index for diagnosing each FL stage: Youden's index=sensitivity + specificity − 1. A probability value of less than 0.05 was considered statistically significant.

Results

Of the 120 rats in this study, pathological results revealed that 42 cases were normal (N) (Fig. 2A), 30 cases had mild FL (L1) (Fig. 2B), 25 cases had moderate FL (L2) (Fig. 2C), and 13 cases had severe FL (L3) (Fig. 2D). Ten rats were excluded from the study. Three of these rats died of unknown causes, 5 of them died as a result of anesthesia accidents, and 2 of them did not have qualified ROIs for RF data analysis.

Means of the four parameters for various degrees of FL are shown in Table 1. Differences in Mean, MSR, SK and KU among the various degrees of hepatic steatosis are shown in Table 2. There were significant differences in the four indexes between the normal control group and the experimental groups ($P<0.05$), and there was a significant difference between the mild and moderate groups and the mild and severe fatty liver groups ($P<0.001$). There was also a significant difference in Mean between the moderate and severe fatty liver groups ($P<0.001$). There were no significant differences in MSR, SK, and KU between the moderate and severe fatty liver groups ($P=0.059$, 0.077, and 0.142, respectively).

Mean, MSR, SK, and KU were significantly correlated with FL grades (r=0.71, $P<0.001$; r=0.81, $P<0.001$; r=−0.79, $P<0.001$; and r=−0.74, $P<0.001$). Stepwise regression analysis was used to narrow the predictors further, and Mean and MSR, with correlation coefficients of 0.71 and 0.81, respectively, were selected for this purpose. The regression equation was $Y=-4.48 + 3.20 \times 10^{-2}X1 + 3.15X2$ ($P<0.001$), where Y=hepatic steatosis grade, X1 =Mean, and X2 =MSR.

Measurements of the diagnostic accuracy of a test using ROC analysis to determine the abilities of the four indexes and combined index (Y) to determine the stage of FL are shown in Figs. 3–5 and Tables 3–7. For Mean, the areas under the ROC curves were 0.83 (L≥L1, $P<0.001$), 0.90 (L≥L2, $P<0.001$), and 0.96 (L≥L3, $P<0.001$), respectively (Table 3). For MSR, the areas under the ROC curves were 0.92 (L≥L1, $P<0.001$), 0.94 (L≥L2, $P<0.001$), and 0.91 (L≥L3, $P<0.001$), respectively (Table 4). For SK, the areas under the ROC curves were 0.92 (L≥L1, $P<0.001$), 0.92 (L≥L2, $P<0.001$), and 0.89 (L≥L3, $P<0.001$), respectively (Table 5). For KU, the areas under the ROC curves were 0.89 (L≥L1, $P<0.001$), 0.90 (L≥L2, $P<0.001$), and 0.87 (L≥L3, $P<0.001$), respectively (Table 6). The areas under the ROC curves of the combined index (Y) were superior to the simple indexes in evaluating hepatic steatosis grade, and they were 0.95 (L≥L1, $P<0.001$), 0.98 (L≥L2, $P<0.001$), and 0.99 (L≥L3, $P<0.001$) (Table 7).

Discussion

Fatty liver, the accumulation of lipids within hepatocytes, is a very common condition. US examination is a simple and convenient method to evaluate FL. Some researchers have tried to improve the accuracy in staging FL by B-mode image features and hepatic vein Doppler waveforms [12, 19]. At present, some new ultrasonic technologies have been applied in diagnosis of liver diseases, including superb microvascular imaging and ultrasound elastography, such as shear wave elastography, FibroScan, and acoustic radiation force impulse imaging. They can be helpful for noninvasive evaluation of fatty liver disease, liver fibrosis, and liver tumors [6, 10, 13, 16]. In recent years, some other researchers have tried to analyze FL by ultrasound RF signals [2, 9, 18, 22].These studies have revealed that there is a strong correlation between the pathology changes of FL and characteristics. Our study derived some parameters from envelope data and analyzed the diagnostic performance of them in FL.

Mean is a parameter representing the average energy of backscattered echo signals. In this study, we found that the value of Mean in FL was higher than that in the normal liver, and it increased gradually from mild to moderate and severe FL. This finding may be due to the incident ultrasound waves interacting with the increased volume of fat granules in FL, and these fat granules may have worked as backscatter particle sources with higher backscatter energy than normal liver tissue. A study by Weijers *et al*. demonstrated that Mean could be used to diagnose FL [21]. Based on our preliminary results,

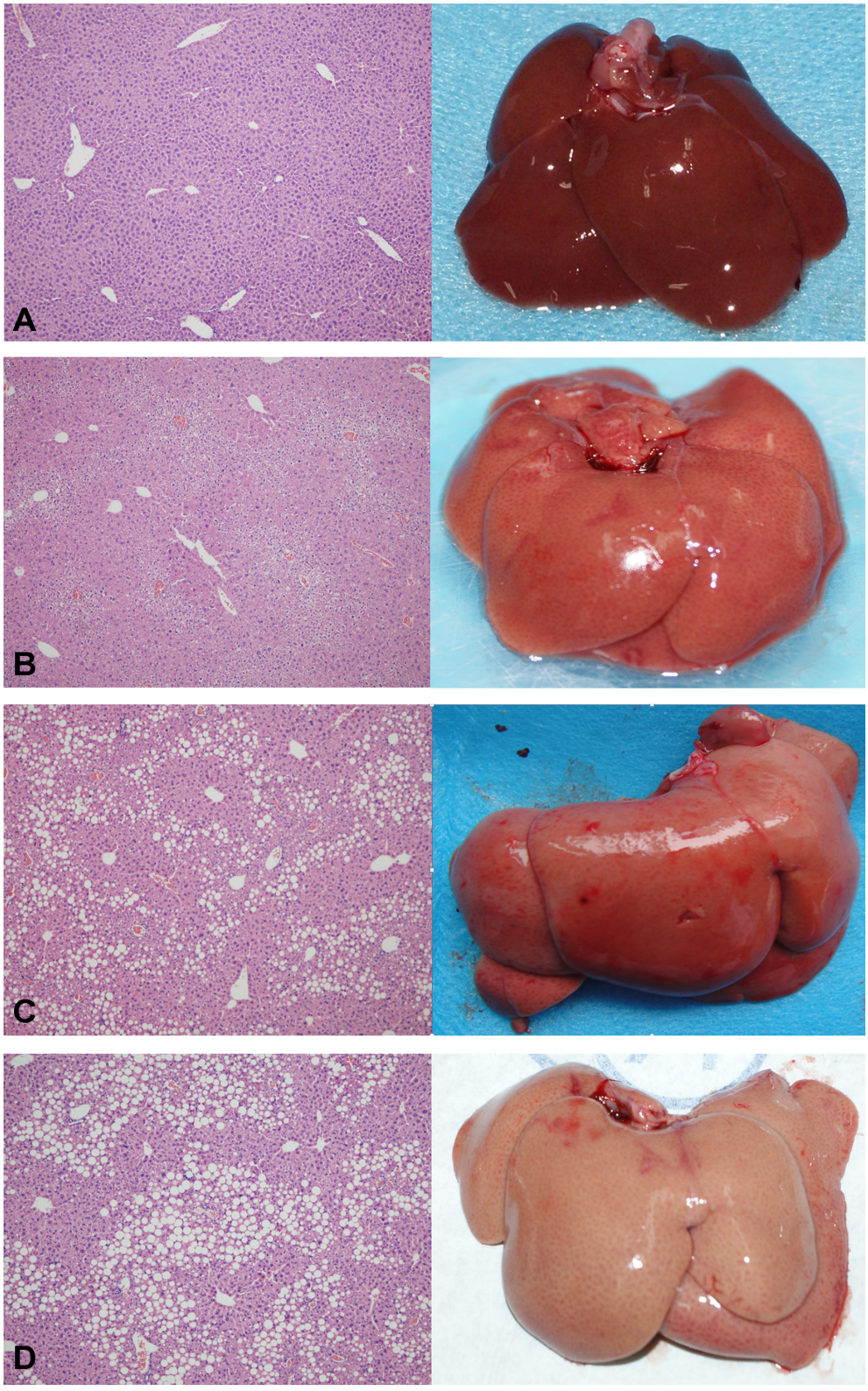

Fig. 2. Images of tissue samples and H&E staining of normal livers and different degrees of fatty liver. a) Tissue sample and H&E staining (×100) of a normal liver. b) Tissue sample and H&E staining (×40) of mild fatty liver. c) Tissue sample and H&E staining (×100) of moderate fatty liver. d) Tissue sample and H&E staining (×100) of severe fatty liver.

Table 1. Four parameters of enveloped time-domain signals in various degrees of FL (mean ± SD)

Group	Number	Mean	Mean/SD ratio	Skewness	Kurtosis
Normal	42	38.93 ± 9.46	1.42 ± 0.12	1.57 ± 0.25	6.20 ± 1.06
Mild	30	44.87 ± 8.67	1.59 ± 0.13	1.22 ± 0.28	5.02 ± 1.04
Moderate	25	57.00 ± 11.20	1.75 ± 0.09	0.94 ± 0.21	4.08 ± 0.82
Severe	13	76.77 ± 13.03	1.83 ± 0.06	0.79 ± 0.09	3.60 ± 0.28

Note: normal, normal control group; mild, mild steatosis group; moderate, moderate steatosis group; severe, severe steatosis group.

Table 2. Differences in Mean, MSR, SK, and KU for various degrees of FL (*P* values)

Group	Mean				MSR				SK				KU			
	Normal	Mild	Moderate	Severe	Normal	Mild	Moderate	Severe	Normal	Mild	Moderate	Severe	Normal	Mild	Moderate	Severe
Normal		0.016	0.000	0.000		0.000	0.000	0.000		0.000	0.000	0.000		0.000	0.000	0.000
Mild	0.016		0.000	0.000	0.000		0.000	0.000	0.000		0.000	0.000	0.000		0.000	0.000
Moderate	0.000	0.000		0.000	0.000	0.000		0.059	0.000	0.000		0.077	0.000	0.000		0.142
Severe	0.000	0.000	0.000		0.000	0.000	0.059		0.000	0.000	0.077		0.000	0.000	0.142	

Note: normal, normal control group; mild, mild steatosis group; moderate, moderate steatosis group; severe, severe steatosis group. Underlining indicates that the statistical results were considered significant. $P<0.05$ was considered to indicate a significant difference.

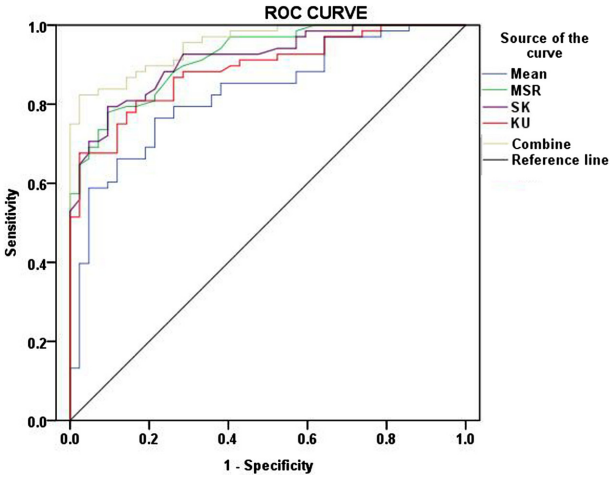

Fig. 3. The ROC curves of the four parameters and combined index (Y) for diagnosing fatty liver (L≥L1). ROC, receiver operating characteristic; MSR, Mean/SD ratio; SK, skewness; KU, kurtosis.

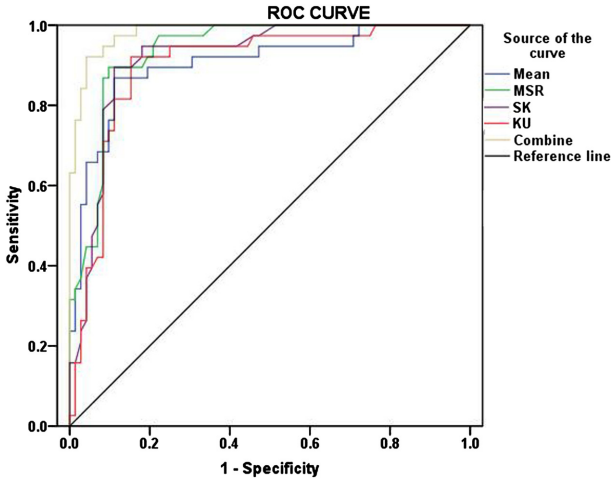

Fig. 4. The ROC curves of the four parameters and combined index (Y) for diagnosing significant fatty liver (L≥L2). ROC, receiver operating characteristic; MSR, Mean/SD ratio; SK, skewness; KU, kurtosis.

Mean is a useful parameter for evaluating various degrees of FL. The ROC analysis also showed that Mean has the potential to detect FL, especially severe FL (AUC=0.96).

MSR represents the relatively homogeneity of the signal amplitude distribution. Generally, the first-order statistics of the amplitude of scattered signals from completely random and highly concentrated scatters are characterized by a Rayleigh distribution in which the MSR is 1.91 [3]. In our study, MSR was significantly different between the FL and normal liver groups. This indicates that the amplitude of time-domain signals of FL was relatively homogeneous and near the envelope with a Rayleigh distribution (MSR=1.91). Our result coincides with the tissue property of FL in which randomly distributed lipid drops makes the density of scatter increase, which causes the scatter distribution to be relatively more homogenous. The ROC results also show that MSR is a useful parameter for diagnosis of FL, es-

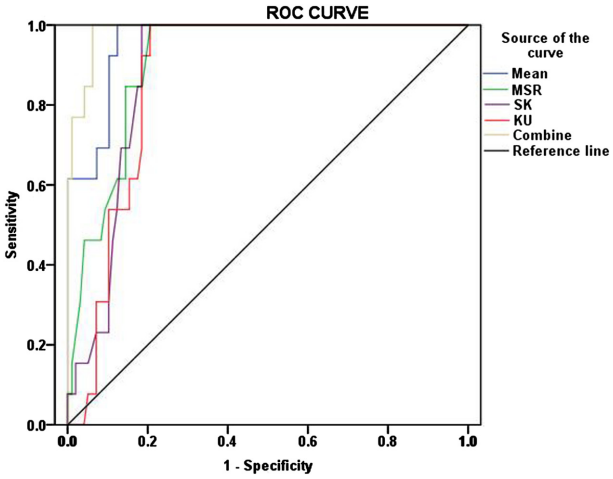

Fig. 5. The ROC curves of the four parameters and combined index (Y) for diagnosing significant fatty liver (L≥L3). ROC, receiver operating characteristic; MSR, Mean/SD ratio; SK, skewness; KU, kurtosis.

pecially significant FL (L≥L2, AUC=0.94). Similar to our results, Weijers *et al*. illustrated that MSR had a good performance in diagnosing FL (AUC=0.94) [21]. Fujii *et al*. showed that MSR had a higher rate of correct diagnosis of FL and cirrhotic liver than B-mode images [2]. In our study, MSR was closely correlated with the FL grades (r=0.81). MSR gradually increased from the normal liver to mild, moderate, and severe FL. Therefore, it may be valuable in estimating the degree of FL quantitatively.

SK and KU are parameters concerning the shape of the envelope data distribution. In our study, SK and KU decreased in order from the normal liver to mild, moderate, and severe FL. Kuc compared the kurtosis in the human normal liver with that in FL [9]. Similarly, the study showed that the kurtosis in FL is lower than in the normal liver [9]. One interpretation of these results is that massive fatty infiltration causes the distribution to be more uniform. The ROC results revealed that SK and KU had a good performance in diagnosing FL. In our study, SK and KU were closely correlated with FL grades (correlation coefficients of −0.79, and −0.74, respectively). Fujii *et al*. revealed that SK and KU were correlated closely with the fibrosis index [2]. SK and KU showed significant differences between the normal liver and mild, mild, and moderate FL. They can distinguish mild FL from moderate and severe FL, but they cannot distinguish moderate FL from severe FL. Our study revealed that the potential of SK and KU to be used in grading of FL.

Table 3. The diagnostic performance of Mean for diagnosing fatty liver

Value	L≥L1	L≥L2	L≥L3
Cutoff value	44.44	52.0	58.0
AUC	0.83	0.90	0.96
Sensitivity (%)	76.5	86.8	100
Specificity (%)	78.6	88.9	87.6

Note: AUC, area under the ROC curve.

Table 4. The diagnostic performance of MSR for diagnosing fatty liver

Value	L≥L1	L≥L2	L≥L3
Cutoff value	1.58	1.68	1.74
AUC	0.92	0.94	0.91
Sensitivity (%)	77.9	89.5	100
Specificity (%)	90.5	90.3	79.4

Note: AUC, area under the ROC curve.

Table 5. The diagnostic performance of SK for diagnosing fatty liver

Value	L≥L1	L≥L2	L≥L3
Cutoff value	1.31	1.10	0.94
AUC	0.92	0.92	0.89
Sensitivity (%)	79.4	89.5	100
Specificity (%)	90.5	88.9	81.4

Note: AUC, area under the ROC curve.

Table 6. The diagnostic performance of KU for diagnosing fatty liver

Value	L≥L1	L≥L2	L≥L3
Cutoff value	4.77	4.75	4.10
AUC	0.89	0.90	0.87
Sensitivity (%)	67.6	92.1	100
Specificity (%)	97.6	84.7	79.4

Note: AUC, area under the ROC curve.

Table 7. The diagnostic performance of the combined index (Y) for diagnosing fatty liver

Value	L≥L1	L≥L2	L≥L3
Cutoff value	1.87	2.42	3.12
AUC	0.95	0.98	0.99
Sensitivity (%)	82.4	92.1	100
Specificity (%)	97.6	95.8	93.8

Note: AUC, area under the ROC curve.

Conventional B-mode ultrasound is the most common technique used to evaluate the presence of fatty liver in clinical practice and many studies. But there are several

limitations of B-mode ultrasound, including subjective evaluation, operator dependency, and limited ability to quantify the amount of fatty infiltration. A meta-analysis study indicated that the overall sensitivity, specificity, and AUC of ultrasound for the detection of moderate to severe fatty liver were 84.8%, 93.6%, and 0.93, respectively [5]. This result is similar to our study. But some research has reported that the sensitivity is low for detecting mild degrees of steatosis, ranging from 55–90%, especially for less than 20–30% steatosis [7]. At the same time, it is said that ultrasound is an unreliable imaging tool for evaluating the degree of fatty liver. However, our study suggested that RF signals can better distinguish mild fatty liver and that the sensitivity of most parameters is more than 75%. More research is needed to evaluate the performance of ultrasound in diagnosis of fatty liver.

Mean and MSR were used to set up a regression equation for predicting hepatic steatosis grade. The regression equation was based on the envelopestatistics, measurement of which was simple and convenient. The ROC analysis results demonstrated that the combined index (Y) expressed by the regression equation was better than the simple indexes for evaluating hepatic steatosis grade. It could be used to make an evaluation of hepatic steatosis grade comprehensive, rapid, and accurate.

The main limitation in this study was that the four parameters we suggested were only extracted in time domain signals. Investigations of the frequency-domain features should be carried out in future RF signal studies. The animal experiment in this in vivo study represents an early stage of this research, and further clinical studies should be carried out the determine the clinical importance of the study findings.

Conclusions

A rat FL model was established, and four time-domain features (Mean, MSR, SK, and KU) were extracted from the ultrasound RF signals of the rat liver, and a regression equation for predicting hepatic steatosis grade was set up. Mean was helpful in differentiating moderate and severe FL. MSR, SK, and KU were valuable in distinguishing normal liver from mild FL, mild FL from moderate FL, and mild FL from moderate and severe FL. The combined index (Y) expressed by the regression equation showed high accuracy in evaluating various degrees of FL. In summary, our study revealed that ultrasound RF signal analysis could possibly be used to grade the degree of severity of rat FL noninvasively. Further clinical study should be carried out to validate our findings.

Conflict of Interest

The authors have no conflicts of interest in connection with this report.

Acknowledgment

This study was supported by the National Natural Science Foundation of China (No. 81501488), Science and Technology Department of Sichuan Province (No. 2017JY0267), and Chengdu Science and Technology Bureau (No. 2014-HM01-00021-SF).

References

1. Bellentani, S., Scaglioni, F., Marino, M., and Bedogni, G. 2010. Epidemiology of non-alcoholic fatty liver disease. *Dig. Dis.* 28: 155–161. [Medline] [CrossRef]
2. Fujii, Y., Taniguchi, N., Akiyama, I., Tsao, J.W., and Itoh, K. 2004. A new system for in vivo assessment of the degree of nonlinear generation using the second harmonic component in echo signals. *Ultrasound Med. Biol.* 30: 1511–1516. [Medline] [CrossRef]
3. Goodman, J.W. 1975. Statistical properties of laser speckle patterns. In: Laser Speckle and Related Phenomena. Topics in Applied Physics, vol 9. *Springer, Berlin, Heidelberg.* 9–75.
4. Haga, Y., Kanda, T., Sasaki, R., Nakamura, M., Nakamoto, S., and Yokosuka, O. 2015. Nonalcoholic fatty liver disease and hepatic cirrhosis: Comparison with viral hepatitis-associated steatosis. *World J. Gastroenterol.* 21: 12989–12995. [Medline] [CrossRef]
5. Hernaez, R., Lazo, M., Bonekamp, S., Kamel, I., Brancati, F.L., Guallar, E., and Clark, J.M. 2011. Diagnostic accuracy and reliability of ultrasonography for the detection of fatty liver: a meta-analysis. *Hepatology* 54: 1082–1090. [Medline] [CrossRef]
6. Kang, B.K., Lee, S.S., Cheong, H., Hong, S.M., Jang, K., and Lee, M.G. 2015. Shear Wave Elastography for Assessment of Steatohepatitis and Hepatic Fibrosis in Rat Models of Non-Alcoholic Fatty Liver Disease. *Ultrasound Med. Biol.* 41: 3205–3215. [Medline] [CrossRef]
7. Khov, N., Sharma, A., and Riley, T.R. 2014. Bedside ultrasound in the diagnosis of nonalcoholic fatty liver disease. *World J. Gastroenterol.* 20: 6821–6825. [Medline] [CrossRef]
8. Komiyama, N., Berry, G.J., Kolz, M.L., Oshima, A., Metz, J.A., Preuss, P., Brisken, A.F., Pauliina Moore, M., Yock, P.G., and Fitzgerald, P.J. 2000. Tissue characterization of atherosclerotic plaques by intravascular ultrasound radiofrequency signal analysis: an in vitro study of human coronary arteries. *Am. Heart J.* 140: 565–574. [Medline] [CrossRef]

9. Kuc, R. 1986. Ultrasonic tissue characterization using kurtosis. *IEEE Trans. Ultrason. Ferroelectr. Freq. Control* 33: 273–279. [Medline] [CrossRef]
10. Kuroda, H., Abe, T., Kakisaka, K., Fujiwara, Y., Yoshida, Y., Miyasaka, A., Ishida, K., Ishida, H., Sugai, T., and Takikawa, Y. 2016. Visualizing the hepatic vascular architecture using superb microvascular imaging in patients with hepatitis C virus: A novel technique. *World J. Gastroenterol.* 22: 6057–6064. [Medline] [CrossRef]
11. Lau, J.K., Zhang, X., and Yu, J. 2017. Animal models of nonalcoholic fatty liver disease: current perspectives and recent advances. *J. Pathol.* 241: 36–44. [Medline] [CrossRef]
12. Lee, C.H., Kim, K.A., Lee, J., Park, Y.S., Choi, J.W., Seo, T.S., and Park, C.M. 2011. Fade-out sign on hepatic tissue harmonic compound sonography: a value as a new sign in the diagnosis of fatty liver. *Eur. J. Radiol.* 80: e258–e262. [Medline] [CrossRef]
13. Lee, D.H., Lee, J.Y., and Han, J.K. 2016. Superb microvascular imaging technology for ultrasound examinations: Initial experiences for hepatic tumors. *Eur. J. Radiol.* 85: 2090–2095. [Medline] [CrossRef]
14. Lee, S.W., Park, S.H., Kim, K.W., Choi, E.K., Shin, Y.M., Kim, P.N., Lee, K.H., Yu, E.S., Hwang, S., and Lee, S.G. 2007. Unenhanced CT for assessment of macrovesicular hepatic steatosis in living liver donors: comparison of visual grading with liver attenuation index. *Radiology* 244: 479–485. [Medline] [CrossRef]
15. Marsman, W.A., Wiesner, R.H., Rodriguez, L., Batts, K.P., Porayko, M.K., Hay, J.E., Gores, G.J., and Krom, R.A. 1996. Use of fatty donor liver is associated with diminished early patient and graft survival. *Transplantation* 62: 1246–1251. [Medline] [CrossRef]
16. Ohno, Y., Fujimoto, T., and Shibata, Y. 2017. A new era in diagnostic ultrasound, superb microvascular imaging: preliminary results in pediatric hepato-gastrointestinal disorders. *Eur. J. Pediatr. Surg.* 27: 20–25. [Medline]
17. Singh, D., Das, C.J., and Baruah, M.P. 2013. Imaging of non alcoholic fatty liver disease: A road less travelled. *Indian J. Endocrinol. Metab.* 17: 990–995. [Medline] [CrossRef]
18. Starley, B.Q., Calcagno, C.J., and Harrison, S.A. 2010. Nonalcoholic fatty liver disease and hepatocellular carcinoma: a weighty connection. *Hepatology* 51: 1820–1832. [Medline] [CrossRef]
19. Uzun, H., Yazici, B., Erdogmus, B., Kocabay, K., Buyukkaya, R., Buyukkaya, A., and Yazgan, O. 2009. Doppler waveforms of the hepatic veins in children with diffuse fatty infiltration of the liver. *Eur. J. Radiol.* 71: 552–556. [Medline] [CrossRef]
20. van Werven, J.R., Marsman, H.A., Nederveen, A.J., Smits, N.J., ten Kate, F.J., van Gulik, T.M., and Stoker, J. 2010. Assessment of hepatic steatosis in patients undergoing liver resection: comparison of US, CT, T1-weighted dual-echo MR imaging, and point-resolved 1H MR spectroscopy. *Radiology* 256: 159–168. [Medline] [CrossRef]
21. Weijers, G., Starke, A., Haudum, A., Thijssen, J.M., Rehage, J., and De Korte, C.L. 2010. Interactive vs. automatic ultrasound image segmentation methods for staging hepatic lipidosis. *Ultrason. Imaging* 32: 143–153. [Medline] [CrossRef]
22. Yamaguchi, T., Zenbutsu, S., Igarashi, Y., Kamiyama, N., Mamou, J., and Hachiya, H. 2010. Echo envelope analysis method for quantifying heterogeneity of scatterer distribution for tissue characterization of liver fibrosis. *IEEE International Ultrasonics Symposium, San Diego*. 1412–1415.
23. Yeh, M.M. and Brunt, E.M. 2007. Pathology of nonalcoholic fatty liver disease. *Am. J. Clin. Pathol.* 128: 837–847. [Medline] [CrossRef]
24. Yokoo, T., Bydder, M., Hamilton, G., Middleton, M.S., Gamst, A.C., Wolfson, T., Hassanein, T., Patton, H.M., Lavine, J.E., Schwimmer, J.B., and Sirlin, C.B. 2009. Nonalcoholic fatty liver disease: diagnostic and fat-grading accuracy of low-flip-angle multiecho gradient-recalled-echo MR imaging at 1.5 T. *Radiology* 251: 67–76. [Medline] [CrossRef]